Science Journal of Energy Engineering
2025, Vol. 13, No. 3, pp. 135-143
https://doi.org/10.11648/j.sjee.20251303.14

SciencePG
Science Publishing Group

Research Article

Numerical Study of a Trapezoidal Tunnel as a Drying Cabin

Mamadou Lamine Coly[1, *], Bou Counta Mbaye[2], Mamadou Seck Gueye[1], Waly Faye[2], Omar Ngor Thiam[2]

[1]Semiconductor and Solar Energy Laboratory, Cheikh Anta Diop University, Dakar, Senegal
[2]Laboratory of Fluid Mechanics, Hydraulics and Transfer, Cheikh Anta Diop University, Dakar, Senegal

Abstract

The drying of fishery products is a critical issue for the valorization of local resources. The most commonly used devices are greenhouse or tunnel dryers, due to their ability to process large quantities of products. In this context, we designed and evaluated a mixed trapezoidal tunnel dryer operating with forced convection, equipped with a solar collector and a drying chamber. This system relies exclusively on solar energy, utilizing both direct solar radiation and the thermal contribution of the collector. To ensure the continuity of the drying process, a stable and constant energy source is required, either through exclusive use of solar energy during the day or with supplementary energy input at night. With this in mind, we investigated the thermal behavior of the drying chamber under steady-state conditions. The objective of this study is to analyze the influence of drying parameters on the heat transfer fluid and the product within a trapezoidal greenhouse dryer. Specifically, we examined the impact of key parameters, such as solar irradiance and air velocity, on the temperature of the heat transfer fluid and the dried product (fish). To this end, a numerical simulation approach was employed to model the thermal behavior of the dryer. The energy conservation equations, derived from the thermal balance of the walls, and the mass conservation equations, based on a polynomial model of the fish drying kinetics, were utilized. The results indicate that the optimal air velocity for effective drying is 1 m/s for low irradiance and 2 m/s for an irradiance of 900 W/m^2. For products with a thickness of approximately 1 mm, the air velocity inside the dryer should not exceed 1 m/s. However, for products with thicknesses ranging from 5 to 20 mm, the air velocity can vary between 1 m/s and 2 m/s. Additionally, for a low irradiance of 300 W/m^2, an air velocity of 0.2 m/s maintains an optimal drying temperature of around 60 ℃. Conversely, for an irradiance of 900 W/m^2, an air velocity of 2.5 m/s is recommended.

Keywords

Dying, Modeling, Simulation, Solar, Thermal, Cabin

1. Introduction

In a context marked by the energy transition and sustainable development, the optimization of solar dryers has become a priority. Solar dryers stand out as an efficient and ecological solution for drying agri-food products. Mathematical modeling, which translates physical phenomena into equations to simulate them using software, is a key method in the study of these devices. It has been applied to various systems, such as greenhouse dryers for residual sludge [1, 2], or agricultural products [3, 4], as well as indirect dryers for agri-food products such as chili pepper [5], tobacco [6] or wood [7, 8]. These

*Corresponding author: mamadouatiamine@gmail.com (Mamadou Lamine Coly)

Received: 28 July 2025; **Accepted:** 11 August 2025; **Published:** 30 August 2025

modeling works generally make it possible to evaluate the thermal performance of the dryers. They can also focus on specific aspects, such as drying efficiency [9, 10] or the impact of parameters influencing the process [11, 12]. Among the notable studies A. Boubeghal and al. numerically analyzed a natural convection solar dryer [13], while Coly and al. modeled a tunnel dryer by simulating transfers in a solar collector [14]. This article proposes to study a trapezoidal greenhouse dryer using modeling and simulation techniques carried out with Python. The approach involves mathematically formulating heat transfer phenomena, including radiative and convective processes, while accounting for physical interactions between the product and the drying chamber. The developed model incorporates a thermal balance across the dryer's compartments and mass transfer processes, based on an empirical model of fish drying kinetics. The objective is to enhance understanding of the thermal dynamics of the heat transfer fluid and the fish within the dryer, thereby optimizing its energy efficiency and overall performance. This work aims to provide valuable insights for improving solar dryer design and advancing their role in sustainable drying solutions.

2. Description of Cabin Components

The drying cabin consists of a horizontal wall and two vertical walls located on either side. Above them, they have a transparent window that acts as a roof. Inside the cabin, there are four racks placed parallel to the horizontal wall (Figure 1). This cabin will function like a greenhouse, converting the direct radiation that passes through the window into heat. The mathematical model of the drying cabin is based on three heat transfer balance equations and one mass transfer equation.

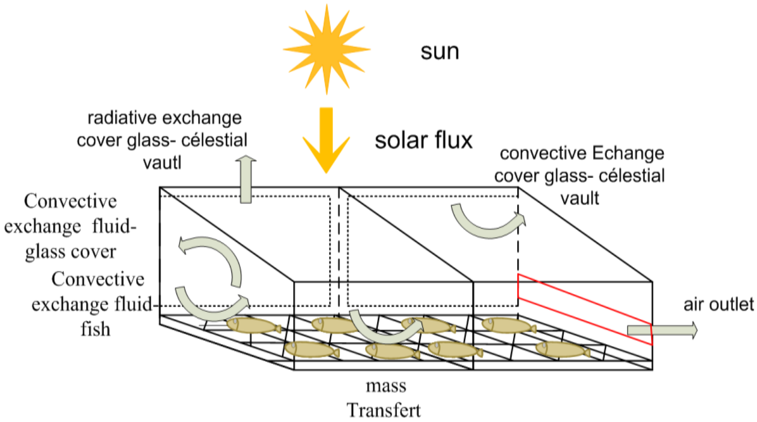

Figure 1. *Heat exchange phenomena in the drying cabin.*

3. Modeling Framework and Governing Equations

3.1. Solar Flux

This is the irradiance received by a wall or element during a given period. The solar irradiance was calculated using climatic design data [15] and represents the incident flux density, expressed in W/m^2 [16]:

At the coverage level:

1. solar flux on the surface of the glass:

$$\varphi_{sol} = \alpha_c S_c G \tag{1}$$

α: Absorption Coefficient

2. solar flux inside the glass:

$$\varphi_{sol} = \alpha_i \varepsilon_i S_i G \tag{2}$$

ε: Reflection Coefficient

3.2. Radiative Flux

These radiative exchanges occur between the various elements inside the dryer, as well as between the cover and the vaulted celestial. Under appropriate assumptions, they can be expressed as follows [17]:

$$\phi_r = h_{r,1-2}(T_1^4 - T_2^4) \tag{3}$$

$h_{r,1-2}$: radiation transfer coefficient between two wall

1. Radiation coefficient between the cover and the vaulted celestial

We *adopt the* relationship proposed in equation (4) [17]:

$$h_{r,c-a} = \sigma.\varepsilon_c\left(\frac{1-\cos\beta}{2}\right) \tag{4}$$

σ: Stephan-Boltzmann Constant Wm^{-2} K^{-4}

2. Temperature of the vaulted celestial

$$T_v = 0.0552 T_{ae} \quad (5)$$

With Tae the ambient air temperature.

3. Radiation coefficient between two walls 1 and 2 [18]

$$h_{r,1-2} = \frac{\sigma}{\frac{1-\varepsilon_1}{\varepsilon_1} + \frac{1}{F_{1-2}} + \frac{1-\varepsilon_2}{\varepsilon_2}\left(\frac{S_1}{S_2}\right)} \quad (6)$$

With F_{1-2} form factor.

3.3. Convective Flow

It describes the heat exchanges between a fluid and a wall, it is defined by [19]:

$$\phi_{c,1-2} = h_{c,1-2} S (T_1 - T_2) \quad (7)$$

$h_{c,1-2}$: radiation transfer coefficient between the cover and the wall

The convection coefficient between the cover and the outside air is calculated by the following Hottel and Woertz relationship [19]:

$$h_{c,c-a} = 5.7 + 3.8 v_{vent} \quad (8)$$

With v_{vent}: average wind speed.

3.4. Convection Coefficient Between the Drying Air and the Walls

This coefficient is determined from the Nusselt number. We will determine the exchange coefficient for each wall of a trapezoidal geometry crossed by air.

$$h_c = \frac{\lambda N_u}{D_n} \quad (9)$$

D_n: a characteristic length for the walls of the dryer.

N_U: the Nusselt number [20]:

$$N_u = 0.019 R_e^{0.8} P_r^{\frac{1}{3}} \quad (10)$$

Re is the Reynolds number defined by [21]:

$$R_e = \frac{V D_n}{\nu} \quad (11)$$

With V: air speed.

$$\nu = 10^{-5}(0.006 T_a + 1.7176) \quad (12)$$

and the number of Prandtl:

Pr = 0.73 for air.

3.5. Experimental Determination of an Equation for the Kinetics of Fish Drying

The moisture loss of the fish was measured at regular intervals during the drying process in a greenhouse, taking into account environmental conditions such as temperature and relative humidity. Based on the experimental data from Coly et al. [14], the drying kinetics $(-\frac{dX}{dt})$ were determined by directly calculating the derivative of the moisture content, there by reflecting the variation in moisture loss over time. Using the Origin Pro software, a trend curve was established (Figure 2), enabling the development of an empirical model (equation (13)) that describes the drying kinetics of the fish in the greenhouse. This empirical model will be incorporated into the heat and mass transfer balance equation (equation (19)) presented in section 3.6.

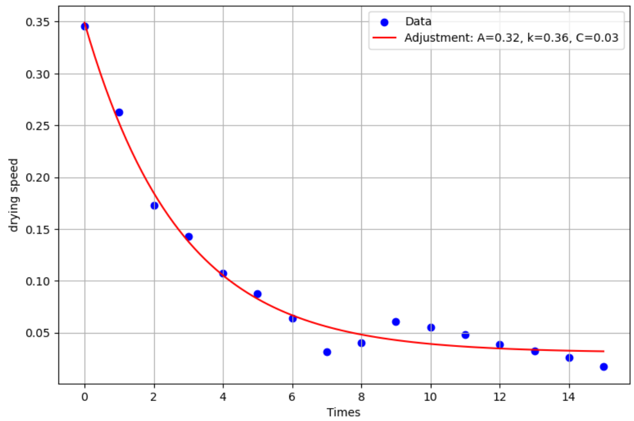

Figure 2. *Trend curve of fish drying kinetics.*

$$-\frac{dX}{dt} = A * exp(-k * t) + C \quad (13)$$

A = 0.32 k = 0.36 C = 0.03

3.6. Presentation of the Mathematical Model of the Drying Cabin

To model our drying cabin, we will make some simplifying assumptions.

Hypotheses:

1) The cover is opaque to IR radiation.
2) The flow is one-dimensional along the longitudinal axis.
3) The temperature of the cover on both sides is uniform.
4) The temperature fields T_c of the cover, T_P of the absorber and T_{pl} of the side wall are uniform.
5) The physical properties of the materials making up the dryer are constant.
6) The ambient temperature is the same around the collector.

7) Thermal exchanges by tray-product conduction are neglected.
8) Shrinkage in the product is neglected.
9) The temperature and water content inside the product are assumed to be uniform.
10) The temperature at the walls is uniform.

We will perform a step-by-step modeling, which involves establishing the heat transfer balance for each component of the cabin, namely the glass cover (equation (15)), the drying air (equation (17)), and the side walls (equation (19)), as well as the heat and mass transfer balance (equation (23)).

1. Coverage balance

$$\varphi_c = \varphi_{sol} - \varphi_{r,c-pr} + \varphi_{c,c-f} - \varphi_{r,c-v} - \varphi_{c,c-a} + \varphi_{r,c-pl} \quad (14)$$

φ_c: heat accumulation flow by thermal inertia of the cover

φ_{sol}: solar flux received by the cover

$\varphi_{r,c-pr}$: heat flow exchanged by radiation between the cover and the products

$\varphi_{c,c-f}$: heat flow exchanged by convection between the cover and the fluid

$\varphi_{r,c-v}$: heat flow exchanged by radiation between the cover and the vaulted celestial

$\varphi_{c,c-a}$: heat flow exchanged by convection between the cover and the outside air

$\varphi_{r,c-pl}$: heat flow exchanged by radiation between the cover and the vaulted celestial

$$\rho_c e_c c_c \frac{dT_c}{dt} = \alpha_v G + h_{c,c-f}\left(T_f - T_c\right) + h_{r,pr-c}\left(T_{pr}^4 - T_c^4\right) + h_{c,c-a}(T_a - T_c) + h_{r,c-v}(T_v^4 - T_c^4) + h_{r,pl-c}\left(T_{pl}^4 - T_c^4\right) \quad (15)$$

$h_{c,c-f}$: convection transfer coefficient between the cover and the fluid

$h_{r,pr-c}$: radiation transfer coefficient between wall and cover

$h_{c,c-a}$: convection transfer coefficient between the wall and the cover

$h_{r,c-v}$: radiation transfer coefficient between the cover and thevaultedcelestial

$h_{r,pl-c}$: radiation transfer coefficient between the side wall and the cover

2. Drying air review

$$\varphi_a = \varphi_{c,f-pr} + \varphi_{c,f-pl} + \varphi_{c,f-c} \quad (16)$$

With:

φ_a: heat accumulation flow by thermal inertia of the air

$\varphi_{c,f-pr}$: heat flow exchanged by convection between the fluid and the product

$\varphi_{c,f-pl}$: heat flow exchanged by convection between the fluid and the side wall

$\varphi_{c,f-c}$: heat flow exchanged by convection between the fluid and the cover

$$D_m c_f \Delta x \frac{dT}{dx} = h_{c,f-pr} S_{pr}(T_{pr} - T_f) + h_{c,f-pl} S_{pl}(T_{pl} - T_f) + h_{c,f-c} S_c(T_c - T_f) \quad (17)$$

$h_{c,f-c}$: convection transfer coefficient between the fluid and the cover

$h_{c,f-pr}$: convection transfer coefficient between the fluid and the product

$h_{c,f-pl}$: convection transfer coefficient between the fluid and the side wall

3. Product thermal balance

$$\varphi_{pr} = \varphi_{c,pr-f} + \varphi_{sol} + \varphi_{r,pl-pr} + \varphi_{r,pr-c} - \varphi_v \quad (18)$$

$\varphi_{r,pl-pr}$: heat accumulation flow by thermal inertia at the product level

φ_v: phase change flow at the product level

$\varphi_{r,pr-c}$: heat flow exchanged by radiation between the product and the cover

φ_{sol}: solar flux received by the product

$\varphi_{c,pr-f}$: heat flow exchanged by convection between the product and the fluid

$$\rho_{pr} e_{pr} c_{pr} \frac{dT_{pr}}{dt} = h_{c,f-pr}\left(T_f - T_{pr}\right) + \alpha\tau G + h_{r,c-pr}\left(T_c^4 - T_{pr}^4\right) + h_{r,pl-pr}\left(T_{pl}^4 - T_{pr}^4\right) - \dot{m} L_V \quad (19)$$

$h_{c,f-pr}$: convection transfer coefficient between the fluid and the product

$h_{r,c-pr}$: radiation transfer coefficient between the cover and the wall

$h_{r,pl-pr}$: radiation transfer coefficient between the side wall and the product

With:

$$\dot{m} = M_s\left(-\frac{dX}{dt}\right) \quad (20)$$

$\dot{m}$: speed of water removal in the product

Ms: dry mass of the product

$$Lv = 4{,}1868(597 - 0{,}56\, T_{p_r}) \quad (21)$$

4. Thermal balance of the walls

$$\varphi_{pl} = \varphi_{sol} + \varphi_{c,pl-f} - \varphi_{r,pl-c} - \varphi_{r,pl-pr} \quad (22)$$

φ_{sol}: solar flux received by the side wall

φ_{pl}: heat accumulation flow by thermal inertia at the level of the side wall

$\varphi_{c,pl-f}$: flow exchanged by convection between the side wall and the fluid

$\varphi_{r,pl-c}$: flux exchanged by radiation between the side wall and the cover

$\varphi_{r,pl-pr}$: flux exchanged by radiation between the side wall and the product

$$\rho_{pl} e_{pl} c_{pl} \frac{dT_{pl}}{dt} = \alpha_{pl} \tau_v G + h_{c,f-pl}(T_f - T_{pl}) + h_{r,c-pl}(T_c^4 - T_{pl}^4) + h_{r,pr-pl}(T_{pr}^4 - T_{pl}^4) \quad (23)$$

$h_{c,f-pl}$: convection transfer coefficient between the fluid and the side wall

$h_{r,c-pl}$: radiation transfer coefficient between the cover and the side wall

$h_{r,pr-pl}$: radiation transfer coefficient between the product and the side wall

4. Results and Discussion

4.1. Interdependence Between the Different Elements of the Dryer

Figure 3 represents the evolution of the temperature of the different components of the dryer during drying at constant speed (V= 0.5). So we imposed a minimum irradiance of 300 W/m^2 (Figure 3-a) and a maximum of 900 W/m^2 (Figure 3-b). We note that the temperature of the walls of the greenhouse dryer varies mainly according to the intensity of the radiation. The temperature of these walls increases rapidly until reaching a thermal equilibrium. Whatever the intensity of the radiation used, we see that at the beginning, the temperature of the air is higher than that of the product, here the convective transfer predominates over that by radiation. After a few hours of drying we observe the opposite effect, here the transfers by radiation are predominant compared to convection which allows to have a thermal equilibrium between the walls.

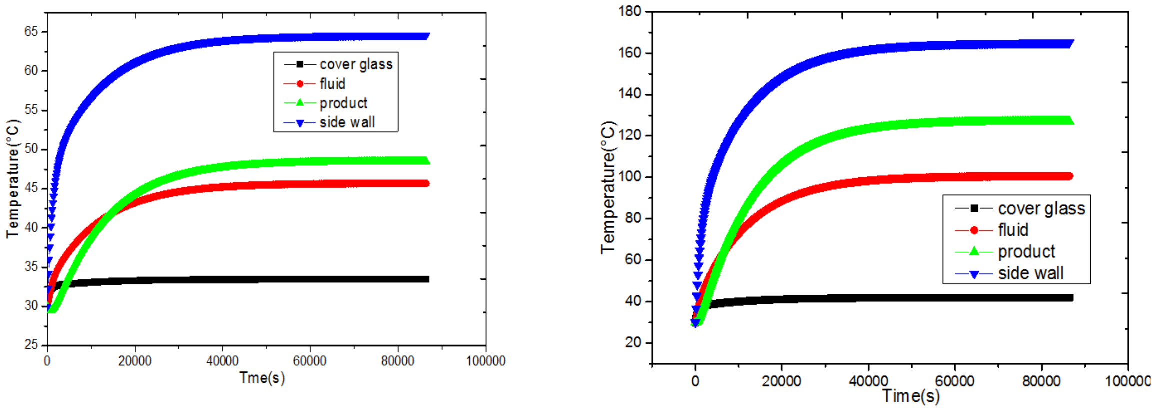

a) Irradiance: G=300 W/m²

b) Irradiance G=900W/m²

Figure 3. Variation of dryer temperature over two extreme conditions.

4.2. Influence of Air Speed on Fluid Temperature

In Figure 4, we have represented the influence of air speed on the fluid temperature for different irradiance values. We see that increasing the air speed promotes the cooling of the dryer components and therefore the fluid temperature. For low speeds (V= 0.05 m/s and 0.5 m/s), the fluid has more time to exchange heat with the materials, which can lead to a higher temperature. On the other hand, a higher speed (v=1 m/s and 3 m/s) increases the heat transfer rate, which can accelerate cooling. However, if the speed is too high (speed above 3 m/s), the fluid will not have enough time to heat the products evenly, which can lead to uneven drying. We also note that when the irradiance is low, around 300 W/m^2, the optimal speed is V=0.2 m/s to have a drying temperature around 60 ℃. On the other hand, if the irradiance is 900 W/m^2, the speed is 2.5 m/s.

Figure 3 illustrates the influence of air velocity on the fluid temperature for various irradiance values. It is observed that an increase in air velocity promotes the cooling of the dryer components, consequently lowering the fluid temperature. At low velocities (V = 0.05 m/s and 0.5 m/s), the fluid has more time to exchange heat with the materials, potentially leading to higher temperatures. Conversely, higher velocities (V = 1 m/s and 3 m/s) enhance the heat transfer rate, which can accelerate cooling. However, excessively high velocities (above 3 m/s) may not allow sufficient time for the fluid to uniformly heat the products, potentially resulting in uneven drying. Additionally, it is noted that at low irradiance levels, approximately 300 W/m^2 (Figure 3-a), an optimal air velocity of V = 0.2 m/s achieves a drying temperature of around 60 ℃. In contrast, at a higher irradiance of 900 W/m^2 (Figure 3-b), the optimal velocity increases to 2.5 m/s.

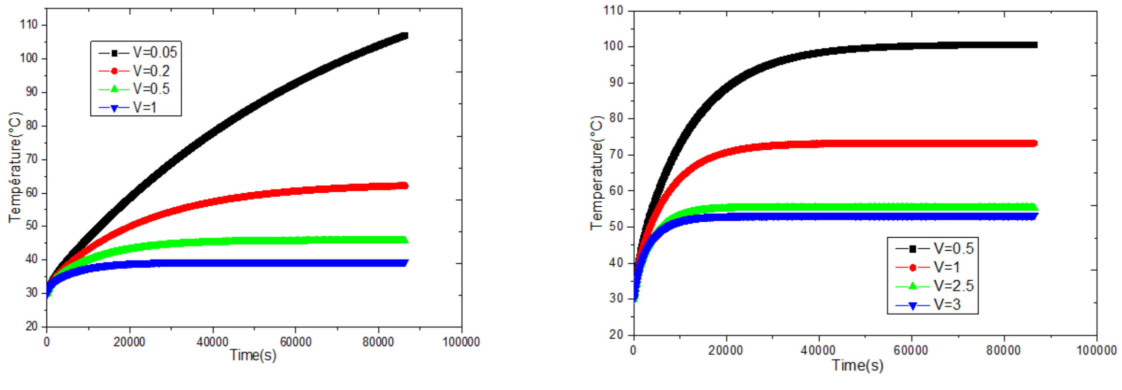

a) Irradiance G=300 W/m²

b) Irradiance G=900W/m²

Figure 4. *Temperature variation over time for different speeds.*

4.3. Influence of Air Speed on Fluid Temperature for Different Product Thicknesses for Irradiance G=700 W/m^2

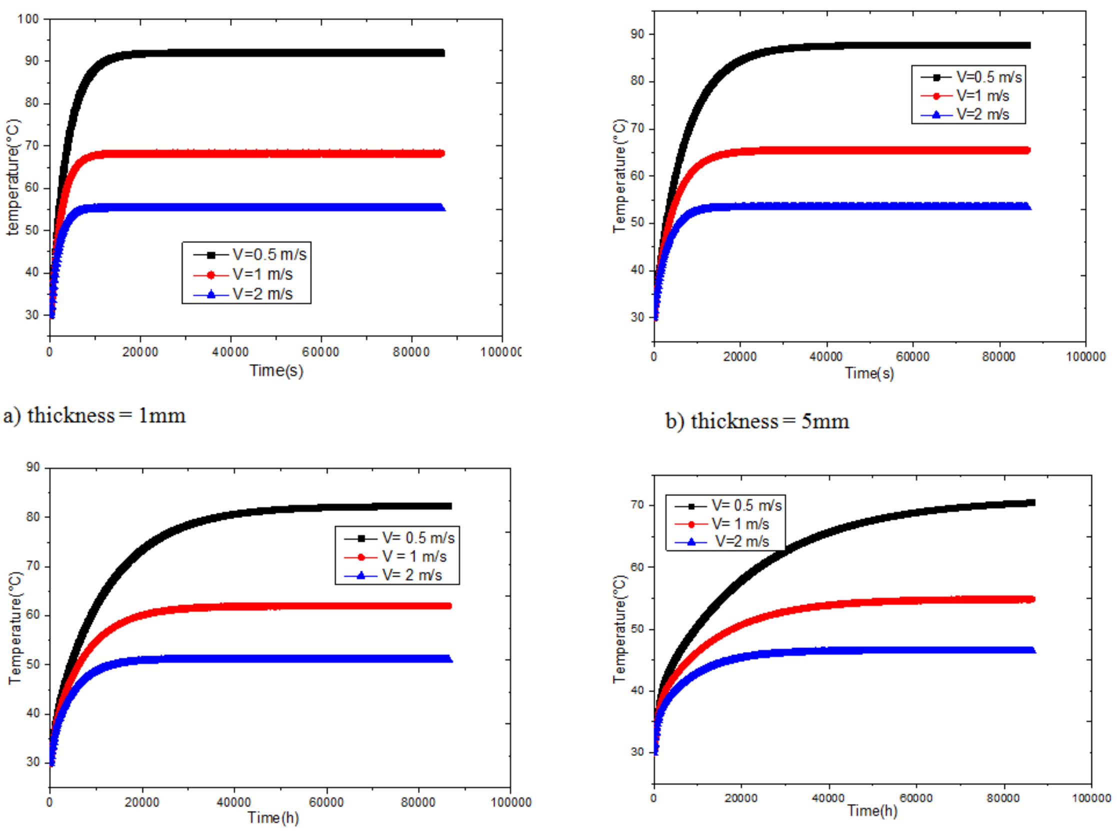

a) thickness = 1mm

b) thickness = 5mm

c) thickness = 10mm

d) thickness = 20mm

Figure 5. *Evolution of the fluid temperature for different product thicknesses.*

In Figure 5, we see that the thickness of the food product and the flow velocity of the fluid strongly influence the temperature of the fluid. We notice that the increase in the thickness of the product within the dryer for constant velocity and irradiance reduces the fluid temperature. Because increased thickness increases the resistance to fluid flow, which can lead to a decrease in fluid temperature due to energy transfer by convection towards the product. For a product with a thin thickness of approximately 1 mm, the air speed inside the dryer must not exceed 1 m/s. On the other hand, for products with a thickness between 5 and 20 mm, the air speed can vary between 1 m/s and 2 m/s.

Figure 5 demonstrates that the thickness of the food product and the fluid flow velocity significantly influence the fluid temperature. It is observed that, for a constant velocity and irradiance, an increase in product thickness within the dryer reduces the fluid temperature (Figure 5a, 5b, 5c, 5d). This occurs because greater product thickness increases resistance to fluid flow, which can lead to a decrease in fluid temperature due to enhanced convective energy transfer to the product. For a product with a low thickness, approximately 1 mm (Figure 5-a), the air velocity inside the dryer should not exceed 1 m/s. In contrast, for products with thicknesses ranging from 5 to 20 mm (Figure 5-b, 5-c, 5-d), the air velocity can vary between 1 m/s and 2 m/s.

4.4. Influence of Irradiance on Fluid Temperature

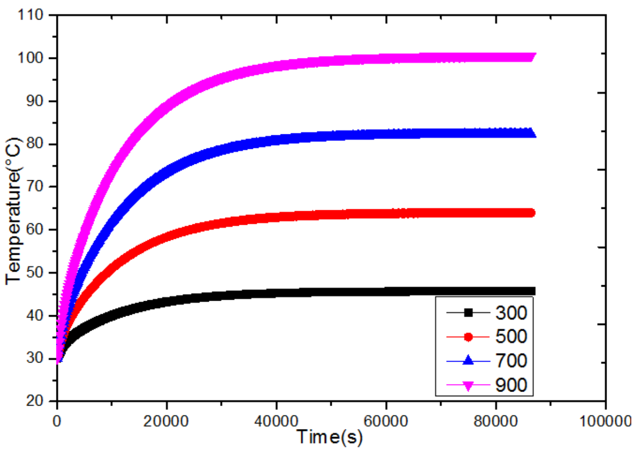

Figure 6. *Fluid temperature variation for different irradiance.*

In Figure 6. we set the air speed to V=0.5 and then varied the irradiance. We found that the irradiance increases the amount of heat absorbed by the dryer walls. This allows the temperature of the fluid to be raised, thus improving drying efficiency. irradiance allows to intensify convection currents in the dryer, facilitating more uniform and efficient heat transfer. The irradiance-heated dryer walls transfer heat to the fluid by convection, further increasing the fluid temperature. Irradiance influences the overall energy balance of the dryer, determining the amount of energy available for the drying process At constant fluid speed, the fluid temperature increases until it reaches a plateau due to thermal equilibrium.

4.5. Influence of Irradiance on Product Temperature

The intensity of solar radiation plays a crucial role in regulating the temperature of fish in a greenhouse dryer. Irradiance increases the amount of heat absorbed by the fish, which we see increases over time before reaching equilibrium (Figure 7). This raises the internal temperature of the dryer, thus speeding up the drying process. The increased temperature due to irradiance intensifies convection currents in the dryer, facilitating more uniform and efficient heat transfer. The irradiance-heated dryer walls transfer heat to the fish by radiation, further increasing the fish's temperature.

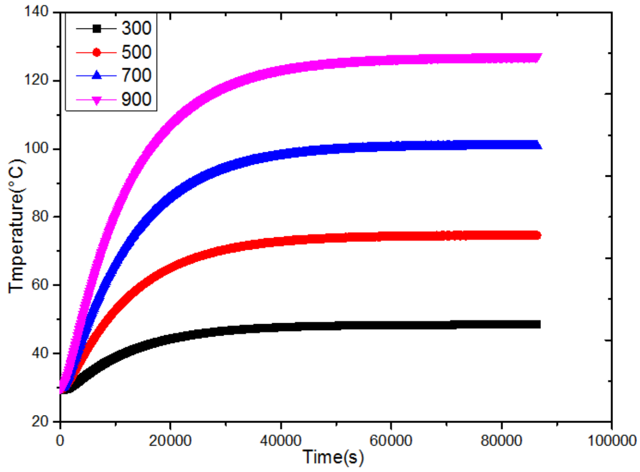

Figure 7. *Variation of product temperature for different irradiance.*

4.6. How the Product Thickness Affects Each Element of the Dryer G=700 for a Constant Speed

Figure 8 illustrates the variation in product temperature over time for different thicknesses at an air velocity of V = 0.5 m/s and an irradiance of G = 700 W/m^2. It is observed that the thickness of the fish in the solar dryer directly affects both the temperature and the drying efficiency. Thicker fish samples exhibit lower temperatures. The fish absorbs energy from the circulating hot air through convection and from surrounding surfaces via radiation. Depending on the thickness, the fish temperature increases until reaching thermal equilibrium. For thicker fish, more time is required for heat to penetrate to the core, which can slow the drying process and necessitate higher temperatures to achieve uniform dehydration. For thinner fish samples (between 1 mm and 5 mm), heat diffusion is faster and more uniform. However, to accelerate drying, it is necessary to increase the air velocity to reduce the risk of overcooking or excessive drying.

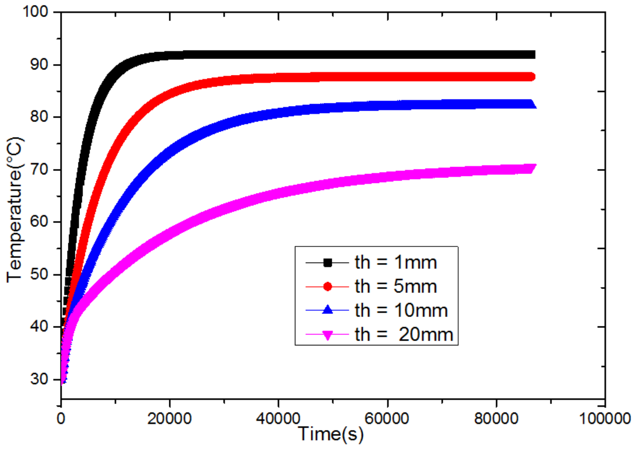

Figure 8. Variation of product temperature over time for different thicknesses.

5. Conclusions

The study carried out on the behavior of the temperature of the fluid and the product in a trapezoidal greenhouse dryer has made it possible to highlight the relevance of this technology in the field of solar drying. Optimizing these parameters helps improve the energy efficiency of the solar drying cabin and the quality of the dried product. Using simulation on different balance equations on python, we were able to identify the key parameters influencing the temperature of the fluid and that of the product. The results obtained showed that the temperature of the different elements of the dryer increases before stabilizing after a certain time for a constant irradiance and speed. The thicker the fish, the lower its temperature. Whatever the irradiance and at constant air speed, the temperature of the fluid and the fish increases until reaching a plateau due to thermal equilibrium. We also note that when the irradiance is low around 300 W/m^2 the optimal speed is V=0.2 m/s to have a drying temperature around 60 ℃. On the other hand, if the irradiance is 900 W/m^2, the optimal speed is 2.5 m/s. For a product with a thin thickness of approximately 1 mm, the air speed inside the dryer must not exceed 1 m/s. On the other hand, for products with a thickness between 5 and 20 mm, the air speed can vary between 1 ms and 2 m/s. These results provide valuable insights into the dynamics of constant-flow drying in this dryer. They can be further validated through subsequent experimental tests on the dryer.

Abbreviations

$c_{\_p}$	Heat Capacity J kg^{-1}. ℃$^{-1}$
G	Irradiance Wm-^{2}
M	Air Mass Flow Rate kg.s^{-1}
$P_{\_th}$	Thermal Power W
$P_{\_n}$	Fan Power W
$S_{\_b}$	Absorber Capture Surface m^2
Sc	Trays Surface m^2
T_P	Absorbent Wall Temperature ℃
T_f	Fluid Temperature at the Dryer Outlet ℃
Tc	Blanket Temperature ℃
t	Drying Time H
T_{pl}	Wall Temperature ℃
α	Absorption Coefficient
β	Tilt Angle Rad
ε	Reflection Coefficient
$\eta_{\_th}$	Thermal Sensor Performances
λ	Air Conductivity W m^{-1}.K^{-1}
ν	Kinematic Viscosity of Air m^2.s^{-1}
ρ	Density kg.m^{-3}
τ	Transmission Coefficient
σ	Stephan-Boltzmann Constant Wm^{-2} K^{-4}

Acknowledgments

This section serves to recognize contributions that do not meet authorship criteria, including technical assistance, donations, or organizational aid. Individuals or organizations should be acknowledged with their full names. The acknowledgments should be placed after the conclusion and before the references section in the manuscript.

Author Contributions

Mamadou Lamine Coly: Conceptualization, Methodology, Writing - original draft

Bou Counta Mbaye: Software, Visualization

Mamadou Seck Gueye: Methodology, Validation

Omar Ngor Thiam: Supervision, Writing - review & editing

Waly Faye: Data curation, Software

Funding

This work is not supported by any external funding.

Data Availability Statement

The data is available from the corresponding author upon reasonable request.

Conflicts of Interest

The authors declare no conflicts of interest.

References

[1] BERROUG, Fatiha, BELLAZIZ, Yassir, TAGNAMAS, Zakaria, et al. Drying Performance of a Combined Solar Greenhouse Dryer of Sewage Sludge. Sustainability, 2024, vol. 16, no. 22, p. 9925.

[2] Slim, R., Zoughaib, A., & Clodic, D. Modeling of a solar and heat pump sludge drying system. International journal of refrigeration, (2008), 31(7), 1156-1168.

[3] C. Monteil, G. Issanchou, M. Amouroux: Energy model of the agricultural greenhouse. Journal of Physics III, EDP Sciences, 1991, 1(3), pp. 429-454. https://doi.org/10.1051/jp3:1991130

[4] AUMPORN, Orawan, ZEGHMATI, Belkacem, CHESNEAU, Xavier, et al. Numerical study of a solar greenhouse dryer with a phase-change material as an energy storage medium. Heat Transfer Research, 2018, vol. 49, no. 6.

[5] MA Hossain, JL Woods, BK Bala, Optimization of solar tunnel drier for drying of chilli without color loss, Renewable Energy, Volume 30, Issue 5,2005, Pages 729-742, ISSN 0960-1481, https://doi.org/10.1016/j.renene.2004.01.005

[6] Nour-Eddine Benaouda, Maiouf Belhamel. Modeling of a solar tobacco drying system in Algeria. Jean-Jacques BEZIAN. JITH 2007, Aug 2007, Albi, France. ENSTIMAC, 5p., 2007, ISBN 978-2-9511591-6-7. <hal-00167361>.

[7] M. El Hisse, M. Fournier. Modeling and simulation of the operation of a dryer solar agri-food. Journal of Applied Physics, 1988, 23(6), pp. 1161-1168. https://doi.org/10.1051/rphysap:019880023060116100

[8] LAMRANI, Bilal and DRAOUI, Abdeslam. Modeling and simulation of a hybrid solar-electrical dryer of wood integrated with latent heat thermal energy storage system. Thermal Science and Engineering Progress, 2020, vol. 18, p. 100545.

[9] Abdelhamid Belghit l*, Mustafa Belahmidi l, Abdellah Bennis l, Bouchra C Boutaleb I, Sauveur Benet: Numerical study of a solar dryer operating in forced convection Rev CLn Therm (1997) 36, 837-8500 Elsevier, Paris.

[10] LAMRANI, Bilal and DRAOUI, Abdeslam. Thermal performance and economic analysis of an indirect solar dryer of wood integrated with packed-bed thermal energy storage system: A case study of solar thermal applications. Drying Technology, 2021, vol. 39, no. 10, p. 1371-1388.

[11] S. Youcef-Ali_, JY Desmons Influence of the aerothermic parameters and the product quantity on the production capacity of an indirect solar dryer Renewable Energy 2007, 32, 496-511.

[12] Coly, ML, Mbaye, BC, Gueye, MS, Thiam, ON, Sarr, J. Modeling and Simulation of a Trapezoidal Solar Collector. Science Journal of Energy Engineering, (2025). 13(2), 62-70. https://doi.org/10.11648/j.sjee.20251302.13

[13] A. Boubeghal*, M. Benhammou, B. Omari, S. Amara, L. Amer, H. Moungar and S. Ouejdi Numerical study of a solar dryer operating in natural convection Renewable Energy Review ICRESD-07 Tlemcen (2007) 315 - 320.

[14] Mamadou Lamine Coly, Mamadou Seck Gueye, Boucounta Mbaye, Waly Faye and Aicha Diamanka (2020); SALT-BASED PRE-TREATED FISH: STUDY OF PROCESSES AND KINETIC DRYING Int. J. of Adv. Res. 8 (October). 2020, 35-44.

[15] ASHRAE. ASHRAE Handbook—Fundamentals. American Society of Heating, Refrigerating and Air-Conditioning Engineers. Climatic Design Information 2021, 14.1-14.XX. ISBN: 978-1-947192-98-2 (SI edition) / 978-1-947192-97-5 (IP edition). Chapter 14.

[16] Modest, MF Radiative heat transfer (3rd ed.). Academic Press. (2013), ISBN: 978-0-12-386944-9 (hardcover) / 978-0-12-386990-6 (eBook), https://doi.org/10.1016/B978-0-12-386944-9.00001-8

[17] Daguenet, M., Ed., Solar dryers: Theory and practice, (1985), UNESCO, Paris, 440-488.

[18] Eshetu Getahun a, b, c, Mulugeta A. Delelec*, Nigus Gabbiyec, Solomon W. Fantac, Petros Demissieb 3 Maarten Vanierschot: Importance of integrated CFD and product quality modeling of solar dryers for fruits 2 and vegetables: A review. Solar Energy 2021, 220, 88-110, https://doi.org/10.1016/j.solener.2021.03.049

[19] Vásquez, J., Reyes, A., Pailahueque, N. Modeling, simulation and experimental validation of a solar dryer for agro-products with thermal energy storage system. Renew. Energy, 2019, 139, 1375-1390. https://doi.org/10.1016/j.renene.2019.02.085

[20] Vengadesan, E., & Senthil, R. A review on recent development of thermal performance improvement methods of flat plate solar water heater. Solar Energy, (2020). 206, 935-961. https://doi.org/10.1016/j.solener.2020.06.05910.1016/j.solener.2020.06.059

[21] White, F. M. (1974). Viscous fluid flow. Journal of Fluid Mechanics, 64(4), 767-768. https://doi.org/10.1017/S0022112074242607

Research Field

Mamadou Lamine Coly: Solar energy systems, Thermal engineering, drying of food products, Heat transfer, Computational fluid dynamics.

Bou Counta Mbaye: Energy efficiency, Solar thermal collectors, Numerical modeling, Sustainable engineering, Fluid mechanics.

Mamadou Seck Gueye: Solar energy systems, Thermal engineering, drying, Heat transfer, Dying, Energy sustainability.

Omar Ngor Thiam: Energy efficiency, Solar thermal collectors, Numerical modeling, Sustainable engineering, Fluid mechanics.

Waly Faye: Solar energy systems, Thermal engineering, drying, Heat transfer, Energy sustainability.